Integrated Transcriptome and Proteome Analysis Reveals Potential Mechanisms for Differential Abdominal Fat Deposition Between Divergently Selected Chicken Lines

Lijian Wang
Northeast Agricultural University
Li Leng
Northeast Agricultural University
Ran Ding
Northeast Agricultural University
Pengfei Gong
Northeast Agricultural University
Chang Liu
Northeast Agricultural University
Ning Wang
Northeast Agricultural University
Hui Li
Northeast Agricultural University
Zhi-Qiang Du
Northeast Agricultural University
Bohan Cheng (chengbohan1027@126.com)

Research article

Keywords: Fat deposition, Transcriptome, Proteome, Chicken, Adipose tissue

Posted Date: July 28th, 2020

DOI: https://doi.org/10.21203/rs.3.rs-38232/v1

Version of Record: A version of this preprint was published at Journal of Proteomics on June 1st, 2021. See the published version at https://doi.org/10.1016/j.jprot.2021.104242.

Abstract

Background: Genetic selection for meat production performance of broilers concomitantly causes excessive abdominal fat deposition, accompanied by several adverse effects, such as the reduction of feed conversion efficiency and reproduction performance. Our previous studies have identified important genes regulating chicken fat deposition, using the Northeast Agricultural University broiler lines divergently selected for abdominal fat content (NEAUHLF) as an animal model. However, the molecular mechanism underlying fat deposition differences between fat and lean broilers remains largely unknown.

Results: Here, we integrated the transcriptome (RNA-Seq) and quantitative proteome (isobaric tags for relative and absolute quantitation, iTRAQ) profiling analyses on abdominal fat tissues from NEAUHLF chicken lines. Differentially expressed genes (466 DEGs) and proteins (231 DEPs) were identified, and enriched in pathways related to fatty acid metabolism, fatty acid biosynthesis, glycerophospholipid metabolism, and PPAR signaling, and in pathways mainly involved in protein processing, endocytosis and lipid metabolism, respectively. Moreover, several key DEGs and DEPs involved in long-chain fatty acid uptake, *in situ* lipogenesis (fatty acid and cholesterol synthesis), and lipid droplets accumulation were discovered, and most of them were up-regulated in the fat line, after integrated transcriptome and proteome analysis.

Conclusions: Together, our findings provided a novel insight into abdominal fat content discrepancy between the fat and lean chicken lines.

Background

The meat-type chickens (broilers) have been intensively selected for fast growth rate and better feed efficiency over the past 70 years. As the most efficient animal production system, broilers can provide cheap and nutritious animal protein for human consumption. In the meantime, series of problems also occur with broiler's fast growth, such as the decline in physiological adaptability, especially abdominal fat deposition. The excessive deposition of abdominal fats is not only unfavorable to the health of broilers, but also causing a huge economic loss to broiler producers [1]. Consequently, to solve excessive abdominal fat deposition in chicken is still an urgent task for broiler breeders all over the world.

Fat deposition in chicken is a complex quantitative trait regulated by multiple genetic and environmental factors. Previous studies showed that many lipid-related genes were differentially expressed in abdominal fat tissues for chickens fed with high-fat or normal diets, such as *IGF2BP1*, which was demonstrated to promote adipocyte proliferation and differentiation [2]. Since 1996, we established two broilers lines based on divergent selection on abdominal fat percentage and plasma very low-density lipoprotein (VLDL) concentration (NEAUHLF) [3], which is an ideal model for studying the molecular basis of adipose tissue growth and development. As a result, we have discovered a number of key genes underlying fat deposition through microarray [4–5] and two-dimensional gel electrophoresis technologies, such as adipocyte fatty acid binding protein (A-FABP) and Apolipoprotein A-I (Apo-AI) [6–7]. However, the

molecular mechanism for abdominal fat deposition differences between fat and lean broiler lines remains unclear.

Recently, with the development of high-throughput sequencing technology, integration of transcriptome and proteome technologies has become an important means and routine to analyze the molecular mechanism of agricultural complex traits in farm animals [8–10].In the present study, we examined the differences of transcriptome and quantitative proteome profiling on abdominal adipose tissues between the two broiler lines at 7 weeks of age. We identified several key DEGs and DEPs potentially involved in long-chain fatty acid uptake, *in situ* lipogenesis (fatty acid and cholesterol synthesis), and lipid droplets accumulation, facilitating our understanding of abdominal fat content differences between chicken lines under divergent selection.

Methods

Animals and samples preparation

Animal work was conducted according to the guidelines for the care and use of experimental animals established by the Ministry of Science and Technology of the People's Republic of China (approval number: 2006 – 398), and was approved by the Laboratory Animal Management Committee of Northeast Agricultural University (Harbin, China). The experimental birds were obtained from the Avian Farm of Northeast Agricultural University (Harbin, Heilongjiang, China). These broilers under divergent selection over 19 generations were employed from Northeast Agricultural University broiler lines divergently selected for high and low abdominal fat content (NEAUHLF), exhibiting a large difference in abdominal fat content as previously described [3]. In total, ten male birds (lean line, n = 5, and fat line, n = 5) at 7 weeks of age from the 19th generation of NEAUHLF were used for RNA-seq and iTRAQ analysis, and these birds were kept under the same environmental conditions and had free access to feed and water. Abdominal fat tissues were collected right after these birds were euthanized by intramuscular injection of pentobarbital (Sigma, St. Louis, MO, USA) (40 mg/kg) under deep anesthesia, and then immediately frozen in liquid nitrogen and stored at -80℃. The detailed information of selected chickens' body weights, abdominal fat weights (AFW) and abdominal fat percentages (AFP) were listed in Table S1.

Transcriptomic data collection and analysis

Total RNA from abdominal fat tissues was extracted using the TRIzol reagent (Invitrogen, New Jersey, NJ, USA), and genomic DNA was removed by DnaseI treatment. RNA purity, concentration and integrity were checked by NanoPhotometer® spectrophotometer (IMPLEN, CA, USA), Qubit® RNA Assay Kit in Qubit® 2.0 Flurometer (Life Technologies, CA, USA), and RNA Nano 6000 Assay Kit of the Bioanalyzer 2100 system (Agilent Technologies, CA, USA), respectively. After removal of ribosomal RNA and cleaning-up of rRNA free residue, the sequencing libraries were generated using the NEBNext® Ultra™ Directional RNA Library Prep Kit for Illumina® (NEB, USA) following the manufacturer's recommendations. cDNA fragments of 150–200 bp in length were selected and purified with the AMPure XP system (Beckman Coulter, Beverly, USA). Then, library quality was assessed by the Agilent Bioanalyzer 2100 system. Finally,

after cluster generation (cBot Cluster Generation System using TruSeq PE Cluster Kit v3-cBot-HS, Illumina), the libraries were sequenced on an Illumina Hiseq 4000 platform, and 150 bp paired-end reads were produced.

After demultiplex and quality filtering of raw data, clean reads were obtained and aligned to the *G. gallus* reference genome assembly using HISAT2 (v.2.0.4) [11]. The mapped reads of each sample were assembled by StringTie (v1.3.1) [12] in a reference-based approach. The software Cuffdiff (v2.1.1) [13], which provides statistical routines for determining gene expression data using a model based on the negative binomial distribution, was used to calculate FPKMs (fragments per kilobase of exon per million fragments mapped). Transcripts with a p-value ≤ 0.01 and fold changes ≥ 1.5 or ≤ 0.67 were assigned as significantly differentially expressed.

Proteomics

Protein was extracted according to Damerval et al [14], checked by SDS-PAGE (Fig.S1) and determined concentration by the Bradford method [15]. Following reduction, cysteine alkylation, and trypsin digestion, total proteins were treated to obtain peptides, and labeled with iTRAQ 8-plex or iTRAQ 4-plex reagents (AB SCIEX, USA), as 113 (LL1), 114 (LL2), 115 (LL3), 116 (LL4), 117 (LL5), 118 (FL1), 119 (FL2), and as 117 (FL3), 118 (FL4), 119 (FL5), respectively. We pooled all samples and labeled as 121 in 8-plex and 4-plex iTRAQ, to calibrate the two iTRAQ experimental data sets. Then, the iTRAQ-labeled peptide mixture was reconstituted and loaded on SCX (strong cation exchange) column, which were subjected to nanoelectrospray ionization, followed by tandem mass spectrometry (MS/MS) in a TripleTOF 5600 system (AB SCIEX, USA).

The MS/MS data were processed with ProteinPilot Software v. 5.0 (AB SCIEX, USA) against *Gallus gallus* database using the Paragon algorithm [16]. The experimental data from tandem mass spectrometry (MS) were utilized to match the theoretical data to identify proteins, which was performed by the search option (with an emphasis on biological modifications). An automatic decoy database search strategy was used to estimate the false discovery rate (FDR) calculated as the false positive matches divided by total matches, using the PSPEP (Proteomics System Performance Evaluation Pipeline Software, integrated into the ProteinPilot Software). The significantly differentially expressed proteins were identified using the following criteria: 1) peptide groups considered for quantification required at least 2 peptides, and a global FDR less than 1% was used; and 2) a fold change ≥ 1.5 or ≤ 0.67 and with p-value ≤ 0.05 (t-test).

RT-qPCR analysis

To validate RNA-Seq results, 20 DEGs with higher expression levels and larger fold changes were validated by RT-qPCR. Ten male birds (n = 5 for each line) from the 19th generation of NEAUHLF were used. Total RNA from abdominal fat tissue was reversely transcribed into cDNA using a PrimeScript™ RT Reagent Kit (Takara, Dalian, China). FastStart Universal SYBR Green Master kit (Roche) and the ABI 7900 PCR detection system were used to perform RT-qPCR. The program began at 95 ℃ for 30 s for activation, followed by 40 cycles of amplification at 95 ℃ for 5 s and 58 ℃ for 30 s. An additional 15 s at 95 ℃, 1 min at 60 ℃, and 15 s at 95 ℃ were performed for the melt curve stage. The housekeeping gene TATA-

Box binding protein (*TBP*) was used as the control. RT-qPCR primer pairs were designed by Primer Premier 6.0 and the detailed information were listed in Table S2. The comparative $2^{-\Delta\Delta Ct}$ method was used to determine the statistical significance.

PRM-MS analysis

To verify the protein expression level obtained by iTRAQ analysis, 10 DEPs with higher expression levels and larger fold changes were selected for validation. Signature peptides for the target proteins were defined according to the iTRAQ data, and only were unique peptide sequences selected for the PRM-MS analysis (Table S3). We randomly selected 6 male birds from the 19th generation (n = 3 for each line) of NEAUHLF, and extracted the proteins from abdominal fat tissues, which were prepared following the iTRAQ protocol. Tryptic peptides were loaded on C18 stage tips for desalting prior to reversed-phase chromatography on an Easy nLC-1200 system (Thermo Scientific).

One-hour liquid chromatography gradients with acetonitrile ranging from 5 to 35% were used, and PRM was performed on a Q-Exactive Plus mass spectrometer (Thermo Scientific). Methods were optimized for collision energy, charge state, and retention times for the most significantly regulated peptides experimentally, using unique peptides of high intensity and confidence for each target protein. The mass spectrometer was operated in positive ion mode and with the following parameters: the full MS1 scan was acquired with the resolution of 70000 (at 200 m/z), automatic gain control (AGC) target values 3.0×10^6, and a 250 ms maximum ion injection times. Full MS scans were followed by 20 PRM scans at 35000 resolution (at m/z 200) with AGC 3.0×10^6 and maximum injection time 200 ms. The targeted peptides were isolated with a 2.0 Th window and fragmented at a normalized collision energy of 27 in a higher energy dissociation (HCD) collision cell. The raw data were analyzed using Skyline (MacCoss Lab, University of Washington) [17] to get the signal intensities of individual peptide sequences.

For PRM MS data, each sample's average base peak intensity was extracted from the full scan acquisition using RawMeat (version 2.1, VAST Scientific). The normalization factor for sample N was calculated as f_N = the average base peak intensity of sample N divided by the median of average base peak intensities of all samples. The area under curve (AUC) of each transition from sample N was multiplied by this factor. After normalization, the AUC of each transition was summed to obtain AUCs at the peptide level. Relative protein abundance was defined as the intensity of a certain peptide.

Gene enrichment analysis

DEGs and DEPs were submitted for the gene ontology (GO) analysis by DAVID (Database for Annotation, Visualization and Integrated Discovery, https://david.ncifcrf.gov/) version 6.8, and the Kyoto Encyclopedia of Genes and Genomes (KEGG) pathway analysis (http://kobas.cbi.pku.edu.cn/kobas3).

Statistical analysis

All data were shown as mean ± SD. Student's t-test was used to compare the differences between two groups, and the threshold of significance was set at $p < 0.05$.

Results

Transcriptome profiling

RNA-Seq generated 77,841,982 to 95,203,262 raw reads for each library (Table S4). After filtering the low-quality reads, the average number of clean reads was 89,456,223 (99.93%) and 85,002,558 (99.90%) for the lean line (LL) and fat line (FL), respectively (Table S5). Furthermore, the distribution of mapping rates for clean reads to the reference genome ranged from 81.7–86.99%. FPKM was used to estimate the level of gene expression, and a total of 12501 mRNA transcripts (corresponding to 9603 genes) were identified after quality control for each sample. The correlation analysis of the gene expression level between 10 samples was also performed (Fig.S2). Finally, 483 differentially expressed transcripts were found (p-value ≤ 0.01, fold changes > 1.5 or < 0.67), corresponding to 466 genes (DEGs) (Fig. 1a. and Table S6). To verify the accuracy of RNA-Seq data, 20 DEGs were chosen and their expression levels were assayed by RT-qPCR. Except for *MAPK6*, other genes showed consistent results for both RNA-Seq and RT-qPCR (Fig. 1b). Then, GO analysis showed that GO terms, such as "regulation of endocytosis", "cellular response to prostaglandin E stimulus", "filamentous actin" and "nucleolus" were significantly enriched ($p < 0.05$) (Fig. 1c and Table S7), and the KEGG pathway analysis also revealed that these 466 DEGs significantly enriched in 6 pathways, including "fatty acid metabolism", "PPAR signaling pathway", "biosynthesis of unsaturated fatty acids", "metabolic pathways" and "glycerophospholipid metabolism", "fatty acid biosynthesis" ($p < 0.05$) (Fig. 2a and Table S8). Thus, transcriptome sequencing found that pathways related to fatty acid metabolism could be important in fat deposition differences in our divergently selected chicken lines.

iTRAQ-based Proteomics

To better understand the potential mechanisms underlying differential abdominal fat deposition between fat and lean broilers, iTRAQ-based proteomics was also performed. Eight-plex iTRAQ generated 61,498 spectra and 18,672 unique peptides (matching to 2,424 proteins); four-plex iTRAQ generated 45,203 spectra and 14,300 unique peptides (matching to 2,185 proteins). In addition, after stringent selection of unique peptides (95% confidence limit and global FDR < 1%), we identified 2,137 and 1,727 proteins in the two iTRAQ experiments, respectively. There were 1,470 overlapped proteins, which were considered as credible proteins, and those with a fold change of > 1.5 or < 0.67, and p-value ≤ 0.05 were defined as differentially expressed proteins (DEPs). Finally, 231 DEPs were identified between the two chicken lines, of which 139 were up-regulated and 92 down-regulated in the lean line (Fig. 3a). The heat map of hierarchical clustering of DEPs was shown in Figure S3, and detailed information about every DEP was listed in Table S9. To validate the iTRAQ data, we selected 10 DEPs for the PRM analysis, and 9 of 10 proteins were successfully quantified. The PRM results of these nine proteins were consistent with our iTRAQ data (Fig. 3b).

Next, GO enrichment analysis was performed to determine the function of the DEPs. For the biological process (BP) category, “fatty acid biosynthetic process”, “cell redox homeostasis” and “oxidation-reduction” were significantly enriched. In addition, “extracellular exosome” and “calcium ion binding” were the most representative GO term for the cellular component (CC) and the molecular function (MF), respectively (Fig. 3c and Table S10). KEGG pathway analysis showed that the DEPs were mainly enriched in metabolic pathways, protein processing, endocytosis and lipid metabolism-associated pathways, such as PPAR signaling pathway, fatty acid degradation, fatty acid biosynthesis and fatty acid metabolism (Fig. 2a and Table S11). In support of our transcriptome analysis, proteome analysis further discovered that pathways related to fatty acid metabolism are likely important in fat deposition differences between our fat and lean chicken lines.

Integrated transcriptome and proteome analysis

In order to further distinguish the critical DEGs and DEPs that may affect chicken abdominal fat deposition, integrated transcriptome and proteome analysis was conducted by combined analysis on our RNA-Seq and iTRAQ data. First, we obtained a weak positive correlation (Pearson correlation coefficient r = 0.2873, $p < 2.2e\text{-}16$) between the mRNA levels of 962 genes and their corresponding protein levels (Fig. 4a). Among them, 788 (81.91%) were not differentially expressed at either mRNA or protein levels, 117 were not differentially expressed at mRNA level but differentially expressed at proteins, and 35 were not differentially expressed at protein level but differentially expressed at mRNA (Fig. 4b). It was worth noting that 22 genes were differentially expressed at both mRNA and protein levels, showing the same expression tendency (Fig. 4c and Table 1), suggesting these genes could be the key genes involved in the regulation of abdominal fat deposition.

Table 1
Key DEGs and DEPs that may affect chicken abdominal fat deposition

Gene name	Gene symbol	mRNA log_2(LL/FL)	Protein log_2(LL/FL)	Functional annotation
abhydrolase domain containing 12B	ABHD12B	-1.2513	-1.2686	Hydrolase activity
acetyl-CoA carboxylase alpha	ACACA	-0.9520	-0.8905	Fatty acid biosynthesis
acyl-CoA dehydrogenase long chain	ACADL	-0.6277	-	Fatty acid degradation
acetyl-CoA acetyltransferase 1	ACAT1	-	-0.8445	Cholesterol esterification
acyl-CoA oxidase 1	ACOX1	-	-0.6860	Biosynthesis of unsaturated fatty acids
acyl-CoA synthetase long-chain family member 1	ACSL1	-	-2.3066	Fatty acid biosynthesis and uptake
ankyrin 3	ANK3	-1.3682	-0.6159	Protein localization to plasma membrane
annexin A1	ANXA1	-1.3506	-2.0673	Phagocytosis
ADP ribosylation factor like GTPase 6 interacting protein 5	ARL6IP5	-0.6766	-2.2892	L-glutamate transmembrane transport
ATPase, aminophospholipid transporter (APLT), class I, type 8A, member 1	ATP8A1	-1.1905	-0.7780	Phospholipid translocation
carbamoyl-phosphate synthetase 2, aspartate transcarbamylase, and dihydroorotase	CAD	0.7431	0.9193	Cell-cell adhesion
caveolin 1	CAV1	-0.7488	-1.5994	Fatty acids uptake; Lipid droplet accumulation
epoxide hydrolase 2, cytoplasmic	EPHX2	-1.0312	-1.2864	Cholesterol biosynthesis
fatty acid desaturase 2	FADS2	-1.5672	-	Biosynthesis of unsaturated fatty acids

Gene name	Gene symbol	mRNA log_2(LL/FL)	Protein log_2(LL/FL)	Functional annotation
fatty acid synthase	FASN	-	-2.1605	Fatty acid biosynthesis
glypican 4	GPC4	-1.2052	-2.4404	Cell migration
glycerol-3-phosphate dehydrogenase 2, mitochondrial	GPD2	-0.7728	-0.6751	Oxidation-reduction process
glutathione S-transferase theta 1-like	GSTT1L	-0.658	-1.5039	Glutathione metabolic process
3-hydroxyacyl-CoA dehydratase 2	HACD2	-0.8680	-	Biosynthesis of unsaturated fatty acids
lipoprotein lipase	LPL	-	-0.9735	Fatty acids uptake
myosin IC	MYO1C	-0.9474	-2.3242	Vesicle transport along actin filament
3-oxoacyl-ACP synthase, mitochondrial	OXSM	-1.0310	-	Fatty acid biosynthesis
peroxisomal trans-2-enoyl-CoA reductase	PECR	-1.0960	-	Biosynthesis of unsaturated fatty acids
phospholipase C, delta 1	PLCD1	-1.0643	-0.6419	Inositol phosphate biosynthesis
perilipin 1	PLIN1	-	-1.6838	Lipid droplet accumulation
perilipin 2	PLIN2	0.9376	-	Lipid droplet accumulation
perilipin-4	PLIN4	-2.2119	-2.4547	Lipid droplet accumulation
cytochrome p450 oxidoreductase	POR	-1.5648	-1.6635	Cholesterol biosynthesis
periostin, osteoblast specific factor	POSTN	1.0694	0.9081	Cell adhesion
palmitoyl-protein thioesterase 1	PPT1	-	1.1048	Fatty acid elongation

Gene name	Gene symbol	mRNA log_2(LL/FL)	Protein log_2(LL/FL)	Functional annotation
retinol saturase	RETSAT	-1.9529	-4.5581	Oxidation-reduction process
stearoyl-CoA desaturase (delta-9-desaturase)	SCD	-3.2302	-1.0587	Biosynthesis of unsaturated fatty acids
steroid 5 alpha-reductase 3	SRD5A3	-1.2821	-1.4037	Oxidation-reduction process
vesicle amine transport 1	VAT1	-0.7527	-0.9828	Oxidation-reduction process
vimentin	VIM	-0.8462	-1.5274	Structural constituent of cytoskeleton

Second, by comparing the pathways obtained after DEGs and DEPs enrichment analysis, we found that there were five overlapped pathways, four of which were related to lipid metabolism, such as fatty acid metabolism, PPAR signaling pathway, fatty acid biosynthesis and biosynthesis of unsaturated fatty acids (Fig. 2a and 2b), including 15 genes that may important for fat deposition. Together, 35 key DEGs/DEPs (22 significantly differentially expressed at both mRNA and protein levels, and 15 genes in overlapped pathways with ACACA and SCD appear twice) that may affect chicken abdominal fat deposition were discovered through our integrated transcriptome and proteome analysis (Table 1).

Discussion

Our fat and lean broilers have similar body weight but acquire a divergent abdominal fat content. So, it is the ideal animal model to study the molecular basis of fat deposition. In the current study, we combined RNA-Seq and iTRAQ techniques on abdominal adipose tissues from 7-week-old FL and LL broilers, and identified a number of key DEGs and DEPs that may affect fat deposition (Table 1). These genes are mainly involved in lipid metabolism associated processes, such as long-chain fatty acids uptake, *in situ* lipogenesis (fatty acid and cholesterol synthesis), and lipid droplets accumulation.

Long-chain fatty acid uptake

In poultry, fatty acids are taken up by the adipose tissue, which mainly come from triglycerides in plasma lipoproteins (such as VLDL) synthesized and packaged by the liver, and also from triglycerides in portomicrons (PM) assembled by long-chain fatty acids in dietary fat [18]. The triglycerides contained in VLDL and PM are hydrolyzed by lipoprotein lipase (LPL) located in adipose tissue-lined endothelial cells

to produce free fatty acids, which can be taken up by adipocytes and then re-esterified and stored in lipid droplet as triglycerides [19]. Previous studies suggested that increased uptake of fatty acids in abdominal adipose tissue is a major cause of obesity in chickens [20]. In general, most cells show less ability in long-chain fatty acid uptake, whereas adipocytes and cardiomyocytes can efficiently and specifically absorb long-chain fatty acids [21]. In the present study, DEG (*CAV1*) and DEPs (LPL, CAV1, and ACSL1) were implicated in long-chain fatty acid uptake. So, we speculate that long-chain fatty acid uptake may play an important role in chicken adiposity.

LPL is considered to be a rate-limiting enzyme in fat accretion in chicken adipose tissue [22], responsible for decomposing triglycerides in VLDL or PM to release free fatty acids. CAV1 was identified as the main plasma membrane fatty acid binding protein in adipocytes that can bind long-chain fatty acids with high affinity [23]. Lack of CAV1 results in the loss of caveolae and defects in long-chain fatty acid uptake in adipocytes [24]. In addition, CAV1 can bind to the long chain fatty acids on the inner leaflet of the lipid bilayer, and transport fatty acids to the subcellular membrane compartment through vesicle-mediated transport [25]. ACSL1 is an acyl-CoA synthetase, and functions as long-chain fatty acid transport protein in adipocyte [26]. The first step in using long-chain fatty acids in cells is their esterification reaction with CoA, and this reaction is catalyzed by acyl-CoA synthetase (ACS). In humans, there are two related long-chain fatty acid activation-related protein families: fatty acid transporters (FATP) and long-chain acyl-CoA synthetase (ACSLs). ACSL1 was found to co-localize with FATP1 in a small number of 3T3-L1 cells [27]. Furthermore, ACSL1 can promote fatty acid uptake into cells depending on their expression levels [28–29]. In the present study, the expression levels of LPL, ACSL1, and CAV1 were significantly higher in the FL adipose tissue, indicating the adipose tissues of the fat broilers have stronger long-chain fatty acid uptake ability to synthesize more triglycerides.

Fatty acids synthesis

The liver is widely considered to be the main site of *de novo* lipid synthesis in avian species, with more than 70% of *de novo* fatty acid synthesis occurring in liver tissue [30], contradictory to the findings in the present study that a large number of lipogenic genes expressed in chicken abdominal fat tissue. Recent studies have also shown that the lipid synthesis ability of avian adipose tissue may be underestimated. Resnyk et al. [31] performed microarray analysis on 9-week-old chicken abdominal fat tissue and found many genes associated with lipogenesis were highly expressed in fat chicken. Similarly, one RNA-Seq analysis on 7-week-old broilers showed a large number of lipogenic genes were also up-regulated in abdominal adipose tissues from fat chicken [32]. Another RNA sequencing analysis showed that the 7-week-old fast growth chickens (fatter than slow growth chickens) over-express numerous lipogenic genes in adipose tissue, which should enhance *in situ* lipogenesis and ultimately adiposity [33]. Intriguingly, in the present study, we also found several key genes associated with fatty acids synthesis, including DEGs (*ACACA*, *OXSM*, *FADS2*, *SCD*, *PECR*, and *HACD2*) and DEPs (ACACA, FASN, SCD ACSL1, and ACOX1). KEGG analysis showed that ACACA, OXSM, FASN, and ACSL1 were enriched in fatty acid biosynthesis pathway, and FADS2, SCD, PECR, HACD2, and ACOX1 were enriched in the biosynthesis of unsaturated

fatty acids pathway. It is worth noting that two proteins (ACACA and SCD) can work as critical enzymes to synthesize fatty acids. ACACA is the rate-limiting enzyme in fatty acid biosynthesis, which can catalyze the synthesis of malonyl-CoA from two molecules of acetyl-CoA, and produce fatty acids under the action of fatty acid synthase [34]. SCD is a rate-limiting enzyme that catalyzes the formation of monounsaturated fatty acids from saturated fatty acids [35].

Thus, we found that the expression levels of genes related to fatty acid synthesis were significantly higher in the fat line, suggesting the adipose tissues in fat birds have stronger ability of triglycerides synthesis in adipocytes.

Cholesterol synthesis

At the cellular level, the deposition of adipose tissue is the result of the increase of the number of adipocytes (adipogenesis) and the size of single fat cells (triglyceride and cholesterol accumulation in lipid droplets) [36–37].

Adipose tissue is the major site for the storage of cholesterol, containing both free and esterified forms of cholesterol [38]. In the current study, some critical DEGs (*EPHX2* and *POR*) and DEPs (ACAT1, EPHX2, and POR) were related to cholesterol synthesis. ACAT1 is an acetyl-coenzyme A acetyltransferase, which can catalyze the formation of cholesteryl esters from cholesterol and long-chain fatty acyl-CoAs [39]. EPHX2 is a member of the epoxide hydrolase family, and the N-terminal activity of EPHX2 can increase the cell's cholesterol level [40–41]. POR is a microsomal membrane-associated protein of two types: type I and type II, of which type II is responsible for cholesterol synthesis [42]. Lanosterol-14α-demethylase and squalene monooxygenase can participate in cholesterol biosynthesis and require POR as the electron donor [43–44]. EPHX2, POR and ACAT1 were all up-regulated in abdominal adipose tissue of fat line in the current study, suggesting the fat broilers could accumulate more cholesterol to expand the size of adipocytes.

Lipid droplet accumulation

Lipid droplets are dynamic organelles involved in intracellular lipid metabolism in almost all eukaryotic cells, and in white adipocytes, the large unique lipid droplet occupies most of the cell space and volume [45]. Perilipin1 (PLIN1), PLIN2, PLIN4 and CAV1 associated with lipid droplet accumulation were also discovered in the present study. PLINs are proteins that coat lipid droplets in adipocytes, which control the lipolysis of stored neutral lipids by cytosolic lipases. PLIN1 is the most abundant lipid droplet coat protein, and plays a crucial role in restricting adipose lipolysis under basal or fed conditions [46]. However, PLIN2 has minimal control over lipolysis, and may affect lipid droplets accumulation by a different mode. PLIN2 deficient mice can increase triglycerides accumulation in the heart by altered lipophagy [47]. PLIN4 mainly exists in white adipose tissue and is associated with tiny nascent lipid droplets. As a lipid droplet coat protein, PLIN4 can quickly package newly synthesized triacylglycerol, and

store energy to the greatest extent during excessive nutrition [48]. Another lipid droplet coat protein is CAV1, which is an essential component for the assembly of caveola organelles in highly differentiated cells, such as adipocytes. CAV1 usually plays a key structural role in the accumulation of lipid droplets in adipocytes, since the deletion of CAV1 can reduce lipid accumulation, which leads to progressive atrophy of white adipose tissue [49]. PLIN1, PLIN4 and CAV1 were up-regulated and *PLIN2* was down-regulated in the adipose tissue of fat line, indicating that fat birds may accumulate more lipid droplets in adipocytes than the lean birds.

Herein, through the joint analysis of transcriptome and proteome, we found many key genes that may affect chicken fat deposition (Table 1). The differential expression and molecular function of these genes likely lead to the differential accumulation of abdominal fat content, although some of them have not been reported to be directly related to adiposity, such as amino acid metabolism-related genes (ARL6IP5 and GSTTL1) and oxidation-reduction-related genes (SRD5A3, GPD2, RETSAT and VAT1). Functions of these genes in adipose tissue development and fat deposition awaits further investigation.

Conclusion

In summary, molecular differences related to long-chain fatty acid uptake, *in situ* lipogenesis (fatty acid and cholesterol synthesis), and lipid droplets accumulation were discovered to exist between the fat and lean chicken lines, which may contribute to the striking differences of abdominal fat deposition.

Abbreviations

AFP: Abdominal fat percentages; AFW: Abdominal fat weights; AGC: Automatic gain control; AUC: Area under curve; BP: Biological process; CC: Cellular component; DAVID: Database for Annotation, Visualization and Integrated Discovery; DEGs: Differentially expressed genes; DEPs: Differentially expressed proteins; FDR: False discovery rate; FL: Fat line; FPKMs: Fragments per kilobase of exon per million fragments mapped; GO: Gene ontology; HCD: higher energy dissociation; iTRAQ: isobaric tags for relative and absolute quantitation; KEGG: Kyoto encyclopedia of genes and genomes; LL: Lean line; MF: Molecular function; MS: Mass spectrometry; NEAUHLF: Northeast Agricultural University broiler lines divergently selected for abdominal fat content; PM: Portomicrons; PRM: Parallel Reaction Monitoring; RT-qPCR: Real-time quantitative PCR; SDS-PAGE: Sodium dodecyl sulfate-polyacrylamide gel electrophoresis; VLDL: Very low-density lipoprotein.

Declarations

Acknowledgments

The authors thank the members of Poultry Research Group in College of Animal Science and Technology at Northeast Agricultural University for hatching eggs and laboratory technical analyses.

Funding

This study was supported by China Agriculture Research System (No. CARS-41) and the National 863 project of China (No. 2013AA102501). The funders had no role in study design, data collection and analysis, decision to publish, or preparation of the manuscript.

Availability of data and materials

The transcriptomics datasets generated during the current study are available in NCBI SRA (PRJNA354990), and other data generated or analyzed during this study are included in this published article and its supplementary information files.

Authors' contributions

LJW performed the experiments, analyzed data, drafted and wrote the manuscript. LL, RD and CL participated to the sample collection, and helped perform the experiments. PFG participated in the analysis of data. NW helped design the study. HL, ZQD and BHC contributed to the experimental design and manuscript revision. All authors read and approved the final manuscript.

Ethics approval and consent to participate

All animal work was conducted following the guidelines for the care and use of experimental animals, established by the Ministry of Science and Technology of the People's Republic of China (Approval number: 2006-398), and also approved by the Laboratory Animal Management Committee of Northeast Agricultural University.

Consent for publication

Not applicable.

Competing interests

The authors declare that they have no competing interests.

References

1. Wu GQ, Deng XM, Li JY, Li N, Yang N. A potential molecular marker for selection against abdominal fatness in chickens. Poult Sci. 2006;85:1896–9.

2. Chen J, Ren X, Li L, Lu S, Chen T, Tan L, et al. Integrative analyses of mRNA expression Profile Reveal the Involvement of IGF2BP1 in Chicken Adipogenesis. Int J Mol Sci. 2019;20:2923.
3. Guo L, Sun B, Shang Z, Leng L, Wang Y, Wang N, et al. Comparison of adipose tissue cellularity in chicken lines divergently selected for fatness. Poult Sci. 2011;90:2024–34.
4. Wang H, Li H, Wang Q, Wang Y, Han H, Shi H. Microarray analysis of adipose tissue gene expression profiles between two chicken breeds. J Biosci. 2006;31:565–73.
5. Wang HB, Hui L, Wang QG, Zhang XY, Wang SZ, Wang YX, Wang XP. Profiling of chicken adipose tissue gene expression by genome array. BMC Genom. 2007;8:193.
6. Wang D, Wang N, Li N, Li H. Identification of differentially expressed proteins in adipose tissue of divergently selected broilers. Poult Sci. 2009;88:2285–92.
7. Wu CY, Wu YY, Liu CD, Wang YX, Na W, Wang N, et al. Comparative proteome analysis of abdominal adipose tissues between fat and lean broilers. Proteome Sci. 2016;14:9.
8. Zhang H, Jiang H, Fan Y, Chen Z, Li M, Mao Y, et al. Transcriptomics and iTRAQ-proteomics analyses of bovine mammary tissue with streptococcus agalactiae-induced mastitis. J Agric Food Chem. 2018;66:11188–96.
9. Na W, Wu YY, Gong PF, Wu CY, Cheng BH, Wang YX, et al. Embryonic transcriptome and proteome analyses on hepatic lipid metabolism in chickens divergently selected for abdominal fat content. BMC Genom. 2018;19:384.
10. Xu Y, Qian H, Feng X, Xiong Y, Lei M, Ren Z, et al. Differential proteome and transcriptome analysis of porcine skeletal muscle during development. J Proteomics. 2012;75:2093–108.
11. Kim D, Langmead B, Salzberg SL. HISAT: a fast spliced aligner with low memory requirements. Nat Methods. 2015;12:357–60.
12. Pertea M, Pertea GM, Antonescu CM, Chang TC, Mendell JT. Salzberg SL.StringTie enables improved reconstruction of a transcriptome from RNA-seq reads. Nat Biotechnol. 2015;33:290–5.
13. Trapnell C, Williams BA, Pertea G, Mortazavi A, Kwan G, Van MB, et al. Transcript assembly and quantification by RNA-Seq reveals unannotated transcripts and isoform switching during cell differentiation. Nat Biotechnol. 2010;28:511–5.
14. Damerval C, De Vienne D, Zivy M, Thiellement H, Eacute. Technical improvements in two-dimensional electrophoresis increase the level of genetic variation detected in wheat-seedling proteins. Electrophoresis. 2010;7:52–4.
15. Bradford MM. A rapid and sensitive method for the quantitation of microgram quantities of protein utilizing the principle of protein-dye binding. Anal Biochem. 1976;72:248–54.
16. Shilov IV, Seymour SL, Patel AA, Loboda A, Tang WH, Keating SP, et al. The Paragon Algorithm, a next generation search engine that uses sequence temperature values and feature probabilities to identify peptides from tandem mass spectra. Mol Cell Proteomics. 2007;6:1638–55.
17. MacLean B, Tomazela DM, Shulman N, Chambers M, Finney GL, Frewen B, et al. Skyline: an open source document editor for creating and analyzing targeted proteomics experiments. Bioinformatics.

2010;26:966–8.

18. Griffin H. Hermier D.Leanness in domestic birds: Plasma lipoprotein metabolism and fattening in poultry. In: Leclercq B, Whitehead CC. ,editors.Butterworth. London: Academic; 1988. pp. 175–201.
19. Ramenofsky M. Bird migration:Fat storage and fat metabolism in relation to migration. In: Gwinner E, editor. Springer. Berlin/Heidelberg: Academic; 1990. pp. 214–31.
20. Leclercq B, Hermier D, Guy G, Salichon MR, Quignard-Boulangé A, Ardouin B, et al. Evidence of enhanced storage capacity in adipose tissue of genetically fat chickens. J Nutr. 1989;119:1369–75.
21. Schaffer JE, Lodish HF. Molecular mechanism of long-chain fatty acid uptake. Trends Cardiovasc Med. 1995;5:218–24.
22. Sato K, Akiba Y, Chida Y, Takahashi K. Lipoprotein hydrolysis and fat accumulation in chicken adipose tissues are reduced by chronic administration of lipoprotein lipase monoclonal antibodies. Poult Sci. 1999;78:1286–91.
23. Trigatti BL, Anderson RG, Gerber GE. Identification of caveolin-1 as a fatty acid binding protein. Biochem Biophys Res Commun. 1999;255:34–9.
24. Pohl J, Ring A, Ehehalt R, Schulze-Bergkamen H, Schad A, Verkade P, et al. Long-chain fatty acid uptake into adipocytes depends on lipid raft function. Biochemistry. 2004;43:4179–87.
25. Meshulam T, Simard JR, Wharton J, Hamilton JA, Pilch PF. Role of caveolin-1 and cholesterol in transmembrane fatty acid movement. Biochemistry. 2006;45:2882–93.
26. Schaffer JE, Lodish HF. Expression cloning and characterization of a novel adipocyte long chain fatty acid transport protein. Cell. 1994;79:427–36.
27. Gargiulo CE, Stuhlsatz-Krouper SM, Schaffer JE. Localization of adipocyte long-chain fatty acyl-CoA synthetase at the plasma membrane. J Lipid Res. 1999;40:881–92.
28. Krammer J, Digel M, Ehehalt F, Stremmel W, Füllekrug J, Ehehalt R. Overexpression of CD36 and acyl-CoA synthetases FATP2, FATP4 and ACSL1 increases fatty acid uptake in human hepatoma cells. Int J Med Sci. 2011;8:599–614.
29. Tong F, Black PN, Coleman RA, DiRusso CC. Fatty acid transport by vectorial acylation in mammals: roles played by different isoforms of rat long-chain acyl-CoA synthetases. Arch Biochem Biophys. 2006;447:46–52.
30. Leveille GA. In vitro hepatic lipogenesis in the hen and chick. Comp Biochem Physiol. 1969;28:431–5.
31. Resnyk CW, Carré W, Wang X, Porter TE, Simon J, Le Bihan-Duval Eet al. Transcriptional analysis of abdominal fat in genetically fat and lean chickens reveals adipokines, lipogenic genes and a link between hemostasis and leanness. BMC Genomics. 2013; 14:557.
32. Resnyk CW, Chen C, Huang H, Wu CH, Simon J, Le Bihan-Duval E, et al. RNA-Seq analysis of abdominal fat in genetically fat and lean chickens highlights a divergence in expression of genes controlling adiposity, hemostasis, and lipid metabolism. PLoS One. 2015;10:e0139549.

33. Resnyk CW, Carré W, Wang X, Porter TE, Simon J, Le Bihan-Duval E, et al. Transcriptional analysis of abdominal fat in chickens divergently selected on bodyweight at two ages reveals novel mechanisms controlling adiposity: validating visceral adipose tissue as a dynamic endocrine and metabolic organ. BMC Genomics. 2017;18:626.
34. Collins JM, Neville MJ, Pinnick KE, Hodson L, Ruyter B, van Dijk TH, et al. De novo lipogenesis in the differentiating human adipocyte can provide all fatty acids necessary for maturation. J Lipid Res. 2011;52:1683–92.
35. Ntambi JM. Regulation of stearoyl-CoA desaturase by polyunsaturated fatty acids and cholesterol. J Lipid Res. 1999;40:1549–58.
36. Kovanen PT, Nikkilä EA, Miettinen TA. Regulation of cholesterol synthesis and storage in fat cells. J Lipid Res. 1975;16:211–23.
37. Rosen ED, Spiegelman BM. Adipocytes as regulators of energy balance and glucose homeostasis. Nature. 2006;444:847–53.
38. Krause BR, Hartman AD. Adipose tissue and cholesterol metabolism. J Lipid Res. 1984;25:97–110.
39. Antalis CJ, Arnold T, Lee B, Buhman KK, Siddiqui RA. Docosahexaenoic acid is a substrate for ACAT1 and inhibits cholesteryl ester formation from oleic acid in MCF-10A cells. Prostaglandins Leukot Essent Fatty Acids. 2009;80:165–71.
40. EnayetAllah AE, Luria A, Luo B, Tsai H-J, Sura P, Hammock BDet. al. Opposite regulation of cholesterol levels by the phosphatase and hydrolase domains of soluble epoxide hydrolase. TJ Biol Chem. 2008;283:36592–8.
41. Domingues MF, Callai-Silva N, Piovesan AR, Carlini CR. Soluble Epoxide Hydrolase and Brain Cholesterol Metabolism. Front Mol Neurosci. 2020;12:325.
42. Aguilar A, De Luca F, Wu S. P450 oxidoreductase expressed in rat chondrocytes modulates chondrogenesis via cholesterol- and Indian Hedgehog-dependent mechanisms. Endocrinology. 2009;150:2732–9.
43. Ono T, Bloch K. Solubilization and partial characterization of rat liver squalene epoxidase. J Biol Chem. 1975;250:1571–9.
44. Debeljak N, Fink M, Rozman D. Many facets of mammalian lanosterol 14alpha-demethylase from the evolutionarily conserved cytochrome P450 family CYP51. Arch Biochem Biophys. 2003;409:159–71.
45. Konige M, Wang H, Sztalryd C. Role of adipose specific lipid droplet proteins in maintaining whole body energy homeostasis. Biochim Biophys Acta. 2014;1842:393–401.
46. Sztalryd C, Brasaemle DL. The perilipin family of lipid droplet proteins: Gatekeepers of intracellular lipolysis. Biochim Biophys Acta Mol Cell Biol Lipids. 2017;1862:1221–32.
47. Mardani I, Tomas Dalen K, Drevinge C, Miljanovic A, Ståhlman M, Klevstig M, et al. Plin2-deficiency reduces lipophagy and results in increased lipid accumulation in the heart. Sci Rep. 2019;9:6909.
48. Wolins NE, Quaynor BK, Skinner JR, Schoenfish MJ, Tzekov A, Bickel PE. S3-12, Adipophilin, and TIP47 package lipid in adipocytes. J Biol Chem. 2005;280:19146–55.

49. Cohen AW, Razani B, Schubert W, Williams TM, Wang XB, et al. Role of caveolin-1 in the modulation of lipolysis and lipid droplet formation. Diabetes. 2004;53:1261–70.

Figures

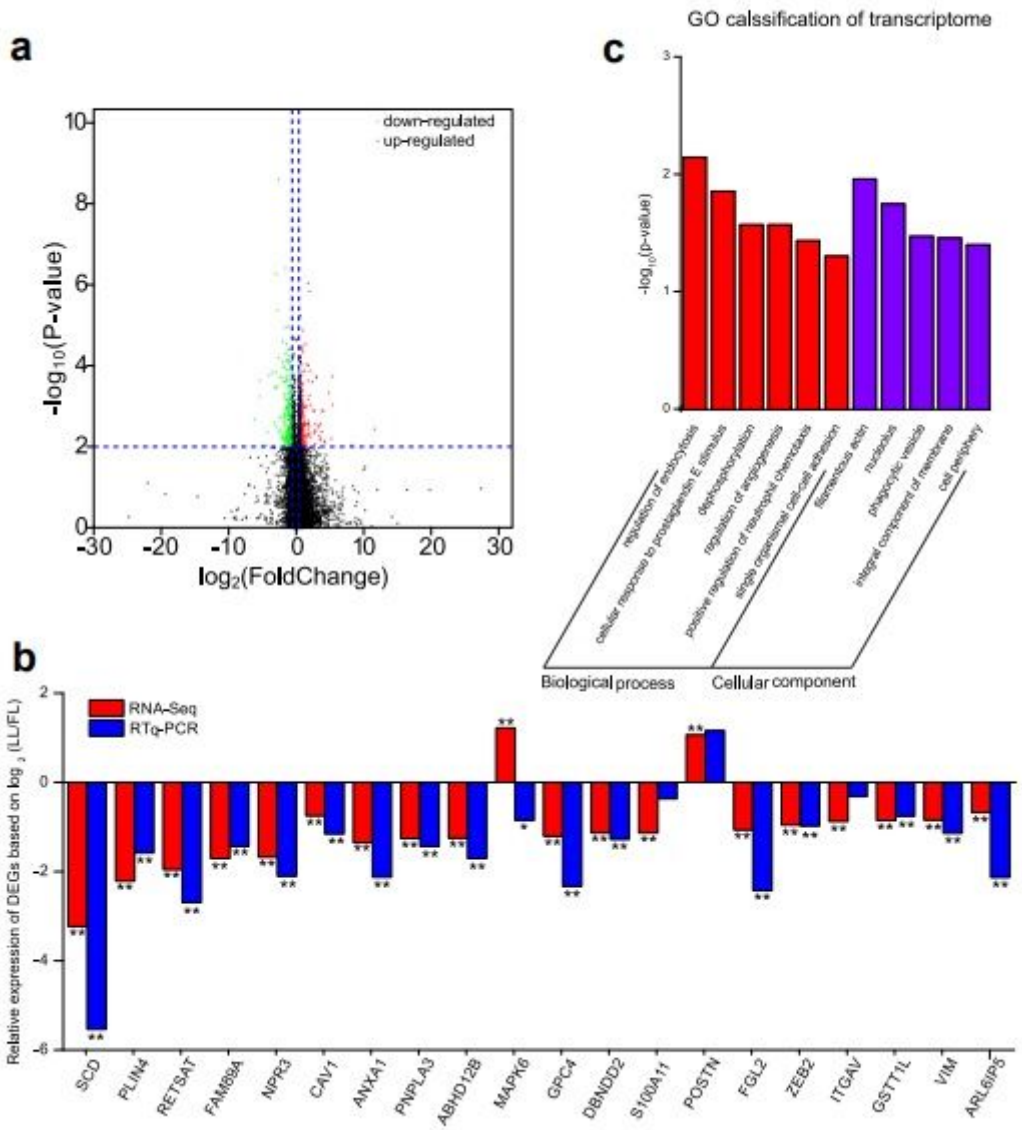

Figure 1

Transcriptome analysis. (a) Volcano plot of DEGs. X-axis shows log2(Fold Change), and Y-axis represents the -log10(p-value). (b) GO analysis of DEGs ($p < 0.05$). X-axis, GO terms, and Y-axis, -log10(p-value). (c) Validation of DEGs by RT-qPCR (n = 5 for each line). * presents $p<0.05$, ** presents $p<0.01$.

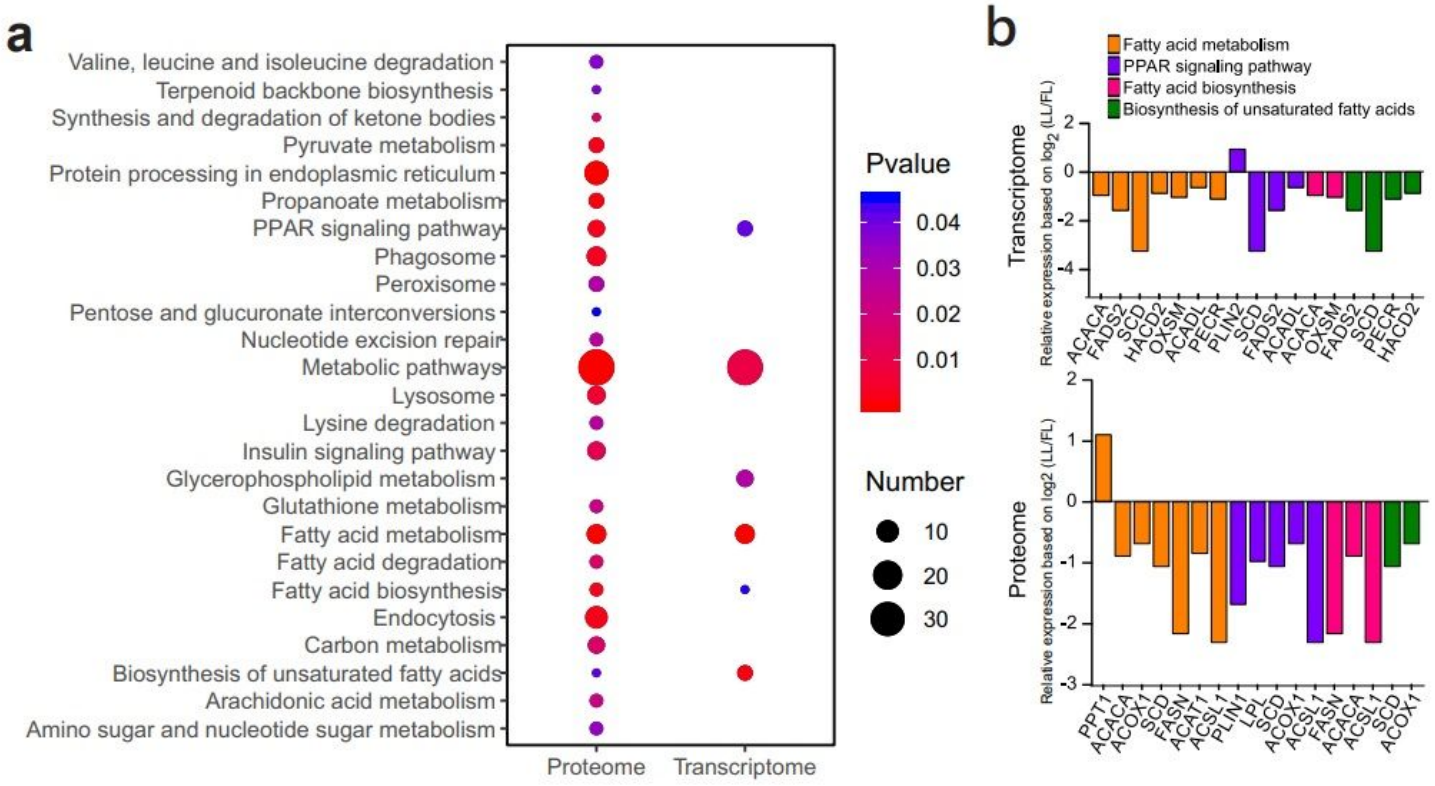

Figure 2

The KEGG analysis of DEGs and DEPs ($p < 0.05$). (a) The overlapped pathways enriched by both DEGs and DEPs. (b) The expression trends of DEGs and DEPs in the four overlapped pathways that related to lipid metabolism.

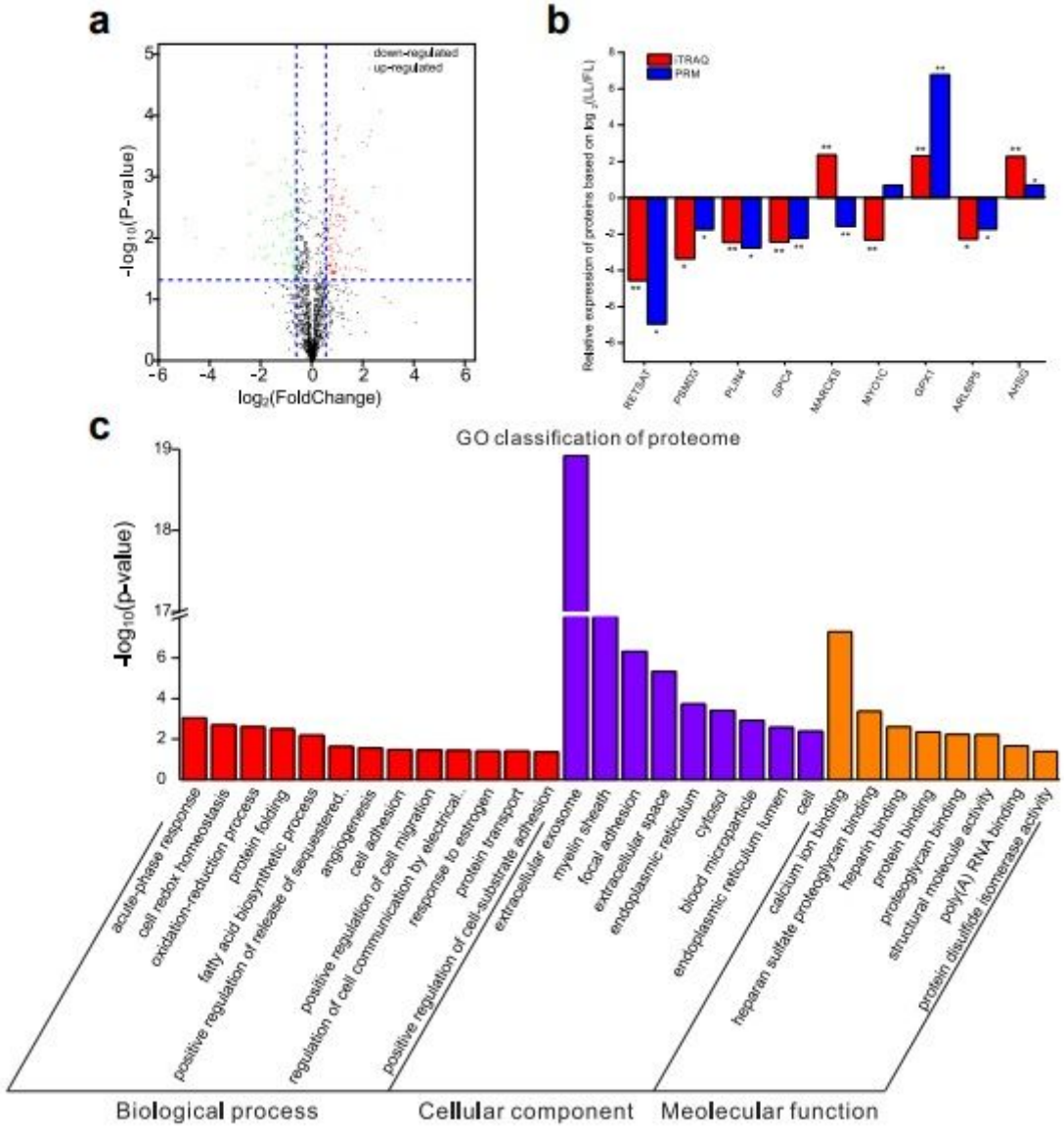

Figure 3

Proteome analysis. (a) Volcano plot of DEPs. X-axis, log2(Fold Change), and Y-axis, -log10(p-value). (b) GO analysis of DEPs ($p < 0.05$). X-axis, GO terms, and Y-axis, -log10(p-value). (c) Validation of DEPs by PRM (n = 3 for each line). * presents $p<0.05$, ** presents $p<0.01$.

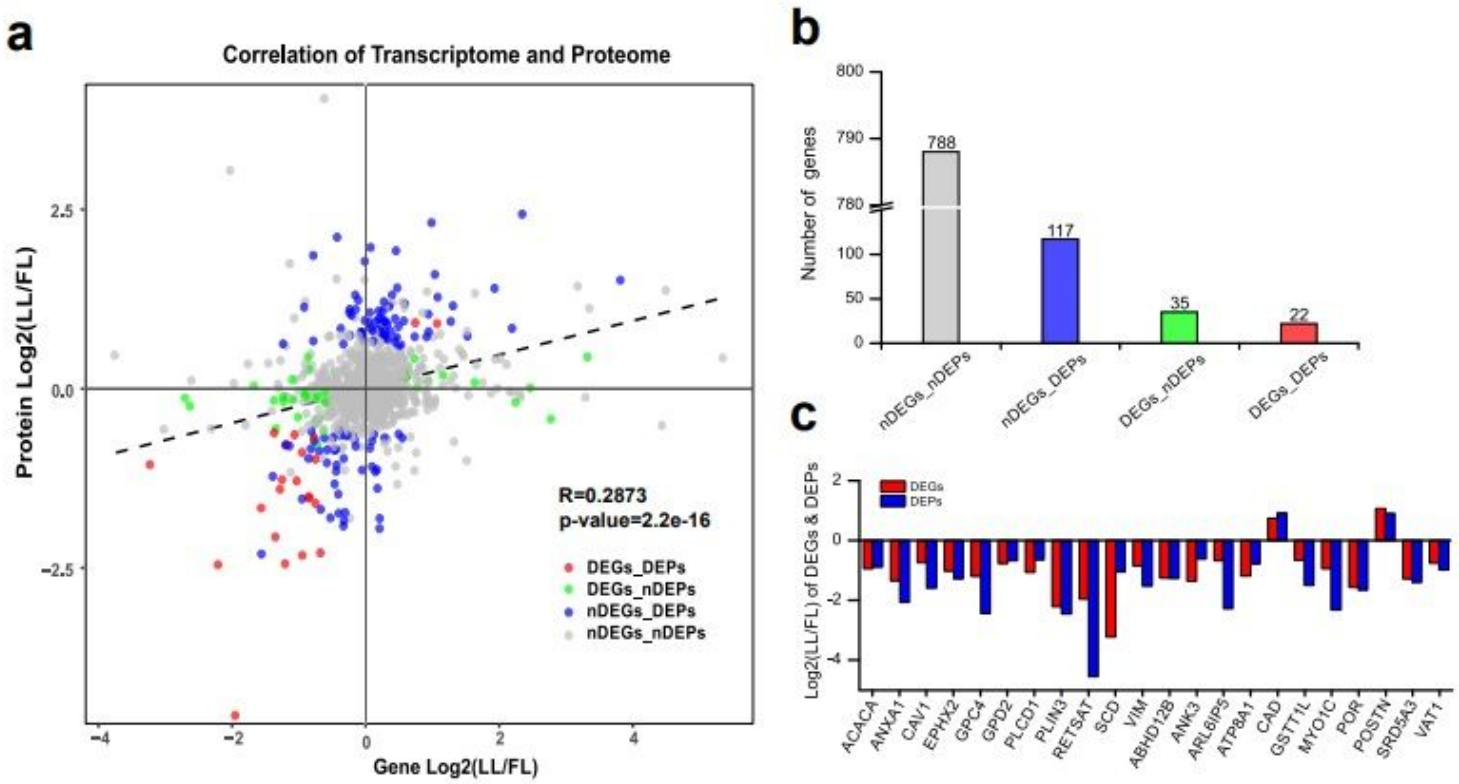

Figure 4

The correlation analysis between transcriptomic and proteomic data. (a) Scatter plots show gene expression at the transcriptional and protein level. Gray dots and nDEGs_nDEPs, genes not differentially expressed at both transcriptional and protein level; Blue dots and nDEGs_DEPs, genes not differentially expressed at the transcriptional level but differentially expressed at protein level; Green dots and DEGs_nDEPs, genes differentially expressed at the transcriptional level but not differentially expressed at the protein level; and red dots and DEGs_DEPs, genes differentially expressed at both transcriptional and protein level. (b) The number of dots for gray, blue, green and red dots. (c) The bar graph shows the expression trends of 22 shared genes (red dots) at both the transcriptional and protein levels.

Supplementary Files

This is a list of supplementary files associated with this preprint. Click to download.

- NC3RsARRIVEGuidelinesChecklist2014.pdf
- TableS11.KEGGpathwaysenrichedbyDEPs.xlsx

- TableS10.GOtermsenrichedbyDEPs.xlsx
- TableS9.DEPsinabdominalfattissues.xlsx
- TableS8.KEGGpathwaysenrichedbyDEGs.xlsx
- TableS7.GOtermsenrichedbyDEGs.xlsx
- TableS6.DEGsinabdominalfattissues.xlsx
- TableS5.Summaryofcleanreadsmappedtogenome.docx
- TableS4.Summaryofsequenceassembly.docx
- TableS3.UniquepeptidesequencesforPRManalysis.docx
- TableS2.PrimersequencesusedforqRTPCR.docx
- TableS1.InformationofchickenbodyweightAFWandAFP.xlsx
- FigureS3.pdf
- FigureS2.pdf
- FigureS1.pdf